

# In situ characterization of formation and growth of high-pressure phases in single-crystal silicon during nanoindentation

Hu Huang<sup>1</sup> · Jiwang Yan<sup>1</sup>

Received: 20 December 2015 / Accepted: 5 March 2016  
© Springer-Verlag Berlin Heidelberg 2016

**Abstract** Pressure-induced intermediate phases of silicon exhibit unique characteristics in mechanics, chemistry, optics, and electrics. Clarifying the formation and growth processes of these new phases is essential for the preparation and application of them. For in situ characterization of the formation and growth of high-pressure phases in single-crystal silicon, a quantitative parameter, namely displacement change of indenter ( $\Delta h$ ) during the unloading holding process in nanoindentation, was proposed. Nanoindentation experiments under various unloading holding loads and loading/unloading rates were performed to investigate their effects on  $\Delta h$ . Results indicate that  $\Delta h$  varies significantly before and after the occurrence of pop-out; for the same maximum indentation load, it tends to increase with the decrease in the holding load and to increase with the increase in the loading/unloading rate. Thus, the value of  $\Delta h$  can be regarded as an indicator that reflects the formation and growth processes of the high-pressure phases. Using  $\Delta h$ , the initial position for the nucleation of the high-pressure phases, their growth, and their correlation to the loading/unloading rate were predictable.

## 1 Introduction

Single-crystal silicon, as an important semiconductor material in scientific research and industrial applications, has received intensive attention from multidisciplinary

researchers [1–6]. Pressure-induced phase transformations of silicon are commonly observed during diamond anvil cell and indentation tests [7–15]. Kinds of intermediate phases induced by a contact load have been reported [16–18], such as Si-II phase ( $\beta$ -tin structure), Si-III phase (body-centered cubic structure with 8 atoms per unit cell), and Si-XII phase (rhombohedral structure with 8 atoms per unit cell). Experimental and theoretical results indicated that these intermediate phases exhibit unique characteristics in mechanics [19], chemistry [6], optics, and electrics [20–22]. For example, the Si-II phase has better plasticity than the diamond cubic phase (Si-I phase), which provides the opportunity for ductile machining of single-crystal silicon [19]. The first-principle calculation showed that the Si-XII phase with a narrow band gap has greater overlap with the solar spectrum than other silicon phases [20, 21], which might exhibit improved absorption across the solar spectrum. The Si-III showed a feature of semimetal [22], which has potential applications in multiple exciton generation and next-generation photovoltaics [23]. However, up to now, it is impossible to prepare a significant quantity of these intermediate phases of silicon at ambient pressure.

To explore their potential applications in electronic products, photovoltaic cells, and microelectro mechanical system (MEMS), clarifying the formation and transformation mechanisms of these intermediate phases under a contact load is undoubtedly very important. On loading to a pressure  $\sim 11$  GPa during nanoindentation, the Si-I phase transforms into a denser metallic Si-II phase [24, 25]. On unloading, the Si-II phase undergoes further transformation into a mixture of Si-XII/Si-III phases or  $\alpha$ -Si phase depending on the unloading conditions [12, 14, 26–28]. Slow unloading is preferred to yield a mixture of Si-XII/Si-III phases whose density is  $\sim 9\%$  less than the Si-II phase, and thus discontinuous displacement appears suddenly,

✉ Jiwang Yan  
yan@mech.keio.ac.jp

<sup>1</sup> Department of Mechanical Engineering, Keio University, Yokohama 223-8522, Japan

namely the pop-out. However, for fast unloading, the Si-II readily transforms into *a*-Si gradually and thus an elbow appears [9, 12]. From this point of view, phase transformations in single-crystal silicon are strongly dependent of the unloading rate. However, the initial position for the nucleation of high-pressure phases (Si-XII/Si-III), their growth with pressure release, and their correlation to the loading/unloading rate are still not clear.

To track the formation and growth processes of nanoindentation-induced high-pressure phases, Ruffell et al. [29] used the cross-sectional transmission electron microscopy (XTEM) to study the residual phases in indents after rapidly unloading at different positions. They proposed a two-step process to describe the formation of high-pressure phases [29]. First, small volumes of high-pressure phases randomly nucleate within the Si-II phase during early stages of unloading and they are seeds for subsequent phase transformations. Second, the rest Si-II phase becomes more unstable on further pressure release after small volumes of Si-XII/Si-III phases have formed, and they further transform into high-pressure phases by rapid growth from these seeds when a critical pressure is reached. When the pressure is released very fast, the high-pressure seeds may have insufficient time to nucleate. Their experimental results and analysis enhanced the understanding of the formation and growth processes of nanoindentation-induced high-pressure phases. However, even if very rapidly unloading was implemented at different positions of unloading, the subsequent XTEM observation was performed on the samples that had been completely unloaded. In that case, small volumes of high-pressure phases might have formed because of the complete pressure release. The real situation may be different from that obtained from their XTEM observations. More importantly, the initial position for the nucleation of high-pressure phases has never been identified in previous studies.

For these reasons, new methods are expected to further investigate the formation and growth processes of nanoindentation-induced high-pressure phases of silicon. In this study, we present a quantitative parameter, the displacement change  $\Delta h$  during the unloading holding process, for in situ characterization of the formation and growth of nanoindentation-induced high-pressure Si-XII/Si-III phases, and its effectiveness will be verified by experiments.

## 2 Experimental

Figure 1a illustrates the experimental diagram. A holding load  $\Delta P$  and a holding interval are introduced in unloading during nanoindentation tests. This unloading holding

process, for simplicity, is just called as holding in the following sections of this paper. The displacement change  $\Delta h$  during holding reflects the time-dependent behavior of silicon, as shown in Fig. 1b. As known from previous studies, phase transformations in single-crystal silicon under a contact load are sensitive to pressure and loading/unloading rate [9, 12, 30], and involve remarkable volume change [27]. For example, the phase transformation from the Si-II phase into Si-XII/Si-III phases results in  $\sim 9\%$  volume expansion, leading to an uplift of the indenter, i.e., displacement change of indenter. The nanoindentation instrument usually has sub-nanometer displacement resolution, which makes it possible to detect this small displacement change of indenter during initial nucleation and subsequent growth of Si-XII/Si-III phases. Therefore, by controlling the holding load  $\Delta P$  and the loading/unloading rate, different  $\Delta h$  may be induced, which has the potential to be used for analyzing the phase transformation processes.

Nanoindentation tests were performed on a nanoindentation instrument ENT-1100 (Elionix Inc., Japan) using a Berkovich indenter. This instrument has a displacement resolution of 0.3 nm, load resolution of 1  $\mu\text{N}$ , and sampling time resolution of 1 ms. An *n*-type single-crystal silicon (100) wafer with a resistivity of 2.0–8.0  $\Omega\text{cm}$  was used. For all nanoindentation tests, the maximum indentation load was the same, 50 mN, and the holding time intervals at the maximum indentation load and at the holding load  $\Delta P$  were the same, 20 s. Different holding loads  $\Delta P$ , 45–0 mN with an interval of 5 mN, were selected. Also, different loading/unloading rates were used: 1, 5, 10, 25, and 50 mN/s. For each holding load  $\Delta P$  and loading/unloading rate, ten groups of nanoindentation tests were performed to obtain reliable results. To exclude the effect of other factors, such as thermal drift, vibration, and noise, all nanoindentation tests were carried out at the same experimental environment, and furthermore comparative analysis was performed.

## 3 Results and discussion

Figure 2a presents selected load–displacement curves under a loading/unloading rate of 1 mN/s and different holding loads  $\Delta P$ , 45–15 mN. In these curves, pop-out did not appear, although they occurred in some other experiments, especially when  $\Delta P$  was small. For example, for  $\Delta P = 10, 5$  and 0 mN, pop-out occurred in all load–displacement curves before or during the holding processes because a low loading/unloading rate and a large indentation load were used here, which promotes the occurrence of pop-out [9]. Figure 2b–h give the displacement–time curves corresponding to different holding loads  $\Delta P$  in

**Fig. 1** **a** Diagram of a nanoindentation test with an unloading holding process and **b** the displacement change  $\Delta h$  during the unloading holding process

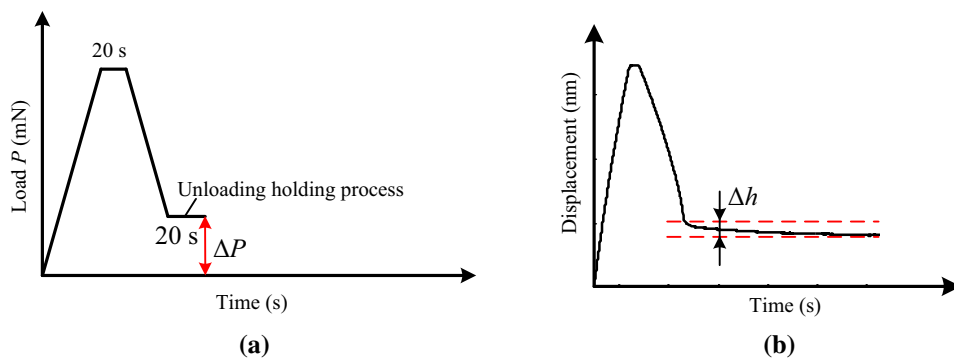


**Fig. 2** **a** Load–displacement curves under different holding loads  $\Delta P$ , and **b–h** displacement–time curves corresponding to different holding loads  $\Delta P$  in Fig. 2a

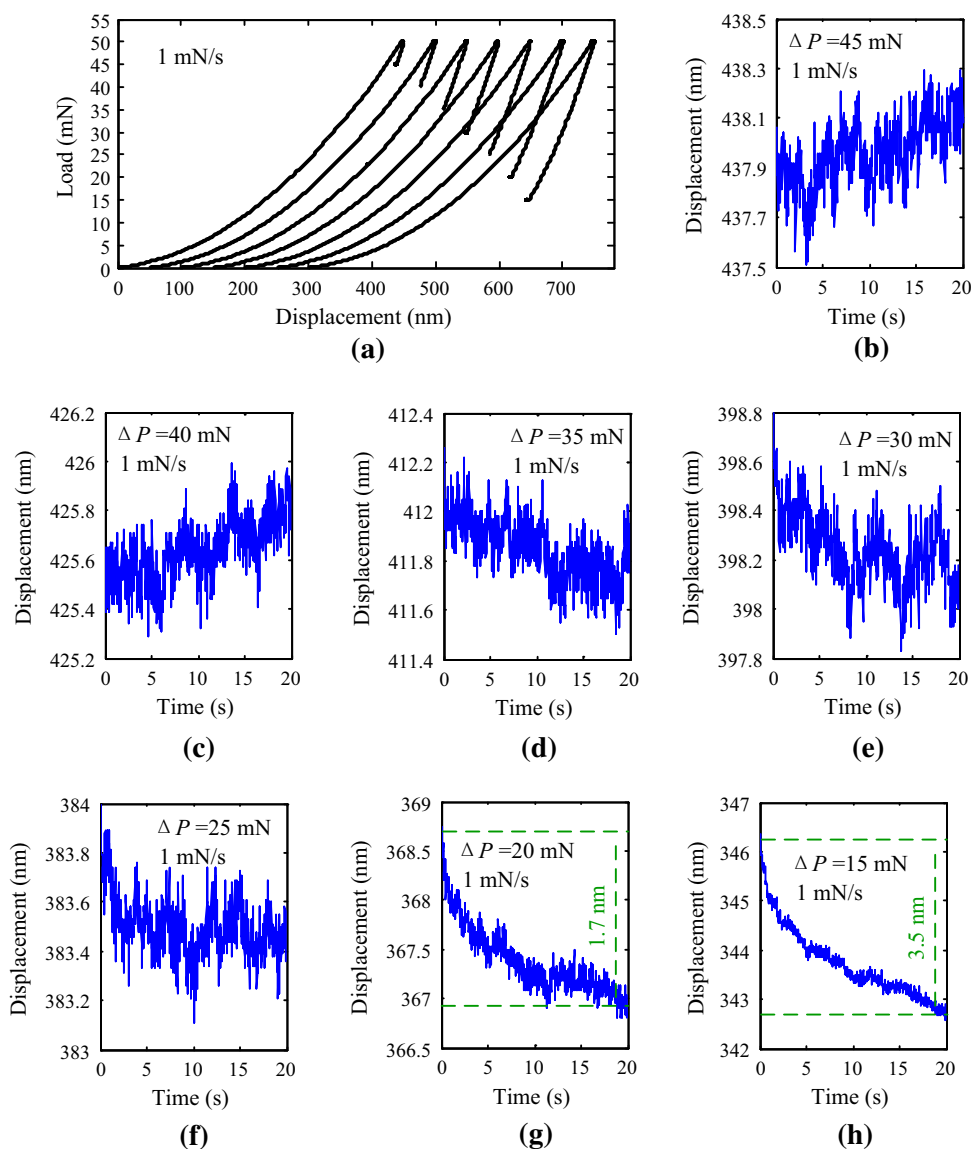


Fig. 2a. In Fig. 2b–f, the displacement change  $\Delta h$  is less than 1 nm during the holding time (20 s). Additionally, the displacement tends to increase in Fig. 2b, c while it tends to decrease in Fig. 2d–f, indicating that the displacement

change in Fig. 2b–c is mainly resulted from the environmental noise or thermal drift. However, in Fig. 2g, h, the displacement change  $\Delta h$  tends to decrease remarkably. For  $\Delta P = 15$  mN, the displacement change  $\Delta h$  reaches

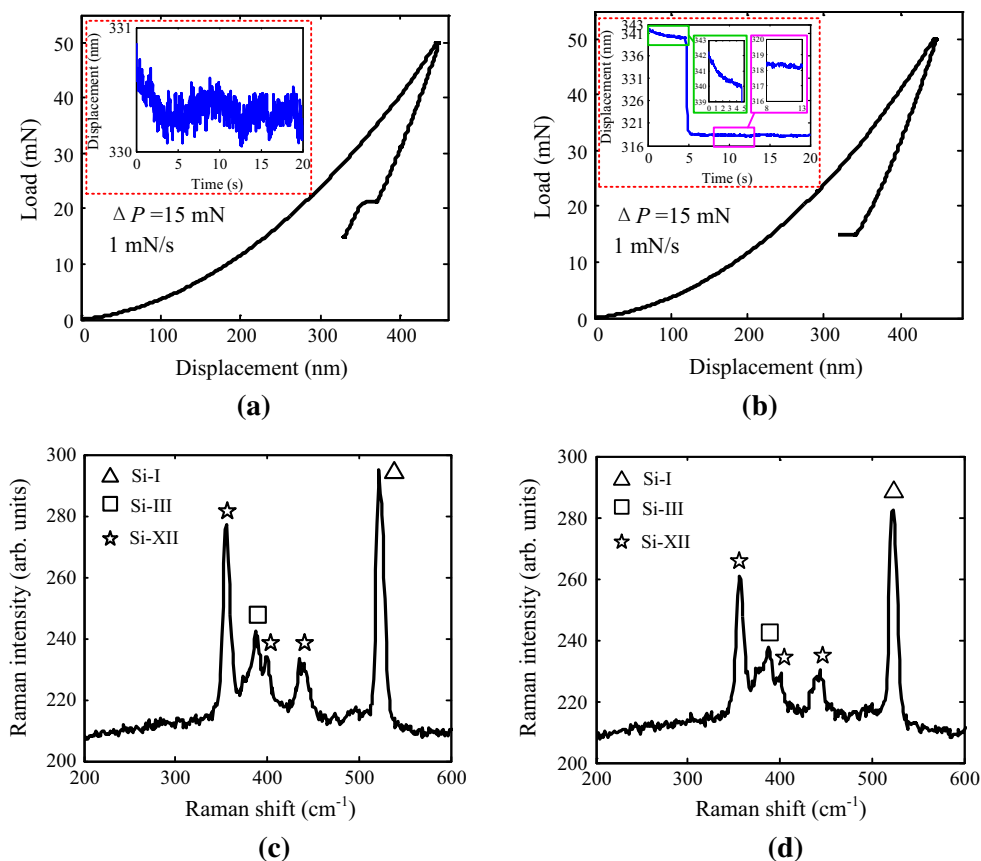
$\sim 3.5$  nm. These results suggest that the indentation displacement is relatively stable during the holding process for a relatively large  $\Delta P$  ( $>20$  mN) but shows remarkable decrease when  $\Delta P$  is less than 20 mN.

Considering the densities of Si-II and high-pressure phases (Si-XII/Si-III), when the Si-II phase transforms into the high-pressure phases, the volume will expand, leading to an uplift of the materials underneath the indenter and decrease in the indentation displacement. Therefore, the remarkable displacement decrease in Fig. 2g, h may denote the occurrence of phase transformation from Si-II into high-pressure phases. Accordingly, the parameter  $\Delta h$  is potentially an indicator reflecting the formation and growth processes of high-pressure phases, especially its initial position. Furthermore,  $\Delta h$  is induced during the phase transformation process, so  $\Delta h$  is a parameter enabling in situ characterization of phase transformation.

To further confirm that the displacement change  $\Delta h$  in Fig. 2g, h is resulted from phase transformation from Si-II into high-pressure phases, Fig. 3a, b give comparative analysis results of two cases under the same indentation conditions: One has a pop-out before the holding process and the other has a pop-out during the holding process. The inserted figures show the displacement–time curves during the holding processes in detail. Figure 3c, d present the

Raman spectra of the residual indents corresponding to the load–displacement curves in Fig. 3a, b, respectively. Similar peaks are observed for these two cases, and Si-XII (peaks at  $\sim 353$ , 397, and 440  $\text{cm}^{-1}$ ) and Si-III (peaks at  $\sim 386$   $\text{cm}^{-1}$ ) phases are identified [31–33]. However, in Fig. 3a, after the pop-out event has occurred, the displacement change  $\Delta h$  is less than 1 nm, which is significantly smaller than that in Fig. 2h ( $\Delta h$  reaches  $\sim 3.5$  nm). This indicates that phase transformation from Si-II into high-pressure phases indeed affects the time-dependent behaviors of single-crystal silicon during the holding process because these two experimental conditions were exactly the same. In Fig. 2h, pop-out did not occur before the holding process, and high-pressure phases could further grow by transformation from Si-II during the holding process, leading to larger volume expansion. Thus, a larger displacement change  $\Delta h$  is observed in Fig. 2(h). However, even the experimental conditions were exactly the same, pop-out has occurred before the holding process in Fig. 3a, which means that phase transformation from Si-II into high-pressure phases has completed. Thus, no further phase transformation occurred during the holding process (no further volume expansion), and the displacement became stable during the holding process. The displacement–time curve during the holding process in Fig. 3b further

**Fig. 3** Load–displacement curves with **a** a pop-out before the holding process and **b** a pop-out during the holding process. The *inserted figures* show the displacement–time curves during the holding processes in detail. **c** and **d** present the Raman spectra of the residual indents corresponding to the load–displacement curves in **(a)** and **(b)**



confirms this displacement change before and after pop-out. In Fig. 3b, the indentation displacement tends to gradually decrease first and then a pop-out occurs at ~5 s, after which the displacement–time curve becomes flat. The comparative analysis results between Figs. 2h, 3a, b indicate a fact that if pop-out has occurred before the holding process, the displacement–time curve becomes flat during the holding process because of no further phase transformation, while if no pop-out appears before the holding process, the indentation displacement gradually decreases during the holding process because of the phase transformation from Si-II into high-pressure phases.

Apart from the results shown in Figs. 2 and 3, in the experiments, we also found that for  $\Delta P = 45\text{--}30$  mN, no pop-out occurs in all load–displacement curves before or during holding processes, but for  $\Delta P = 25, 20,$  and  $15$  mN, pop-out appears in some load–displacement curves before or during holding processes. Combining these results with those in Fig. 2, it can be derived that under the present experimental conditions (maximum indentation load 50 mN, loading/unloading rate 1 mN/s), the initial nucleation of high-pressure Si-XII/Si-III phases happens when the indentation load decreases to ~30 mN. According to the aforementioned results and analysis, Fig. 4 illustrates the initial nucleation and subsequent growth processes of high-pressure Si-XII/Si-III phases during nanoindentation unloading. Considering that it is difficult to distinguish the formation position of Si-XII and Si-III phases individually, they are denoted together as high-pressure Si-XII/Si-III phases. Previous studies by Ruffell et al. [29] suggested that small volumes of Si-XII/Si-III phases are randomly nucleated within the Si-II phase during the early stage of unloading (over 90 % of the maximum load). However, as mentioned in the introduction, their XTEM observation was performed on the samples that had been completely unloaded, and small volumes of high-pressure phases

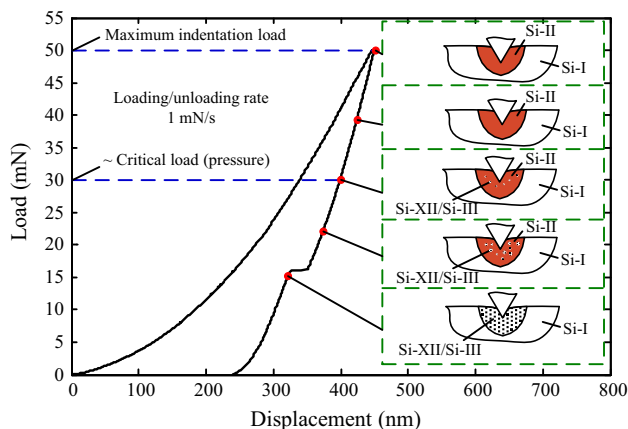


**Fig. 4** Diagram for initial nucleation and subsequent growth processes of high-pressure Si-XII/Si-III phases during unloading

might have formed because of the complete pressure release. The results in this study obtained by in situ characterizing the displacement change  $\Delta h$  during the holding process and observing pop-out events at various holding loads show differences in the initial position for the nucleation of high-pressure phases. Our results imply that the initial nucleation of high-pressure phases is pressure dependent. When the load is released to a critical value (~30 mN in this study, corresponding to ~8 GPa), small volumes of Si-XII/Si-III phases seed within the Si-II phase, rather than randomly nucleate during the very early stage of unloading.

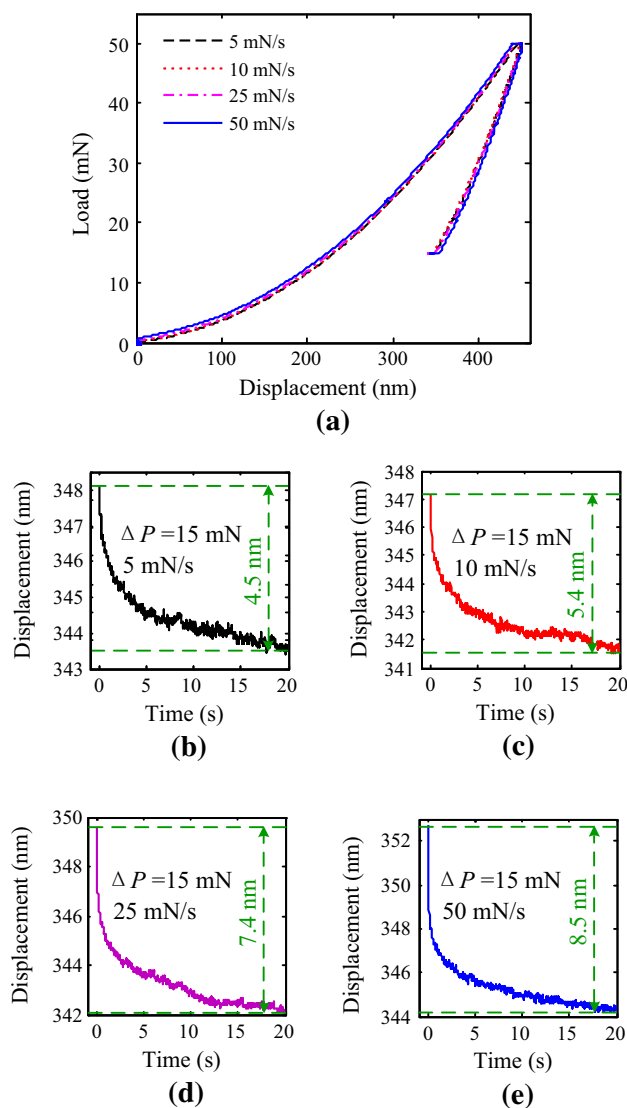


**Fig. 5** a Load–displacement curves under a same holding load  $\Delta P$  but different loading/unloading rates; b–e displacement–time curves during the holding processes corresponding to different loading/unloading rates: b 5 mN/s, c 10 mN/s, d 25 mN/s, and e 50 mN/s

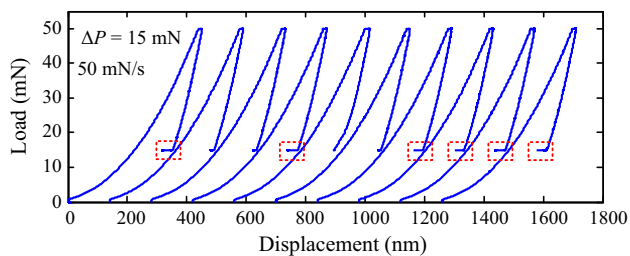


**Fig. 6** Load–displacement curves under a loading/unloading rate of 50 mN/s and a holding load of 15 mN

Figure 5a presents load–displacement curves under a same holding load ( $\Delta P = 15$  mN) but different loading/unloading rates, where no pop-out occurs before or during the holding processes. Although the loading/unloading rate varies from 5 to 50 mN/s, the load–displacement curves agree well with each other. Figure 5b–e give the displacement–time curves during the holding processes corresponding to different loading/unloading rates in Fig. 5a. The displacement change  $\Delta h$  is marked in each figure. From these results and from those in Fig. 2h, it is clear that with the increase in the loading/unloading rate, the displacement change  $\Delta h$  tends to increase, from 3.5 nm for 1 mN/s to 8.5 nm for 50 mN/s. After small volumes of Si-XII/Si-III phases have nucleated within the Si-II phase, they have sufficient time to grow with the pressure release when the unloading rate is low. However, when the unloading rate is very high, the growth of Si-XII/Si-III phases is greatly hindered. The holding process provides a chance for further growth of the high-pressure phases, leading to a larger displacement change in Fig. 5e. Figure 6 gives load–displacement curves at a loading/unloading rate of 50 mN/s, from which it can be seen that the pop-out occurs during holding processes in six groups of experiments. This further indicates that fast unloading limits the growth of high-pressure phases, but random nucleation may still happen when pressure releases to a critical value. If a holding process is provided in this case, high-pressure phases may further grow from previous seeds, leading to occurrence of a pop-out.

## 4 Conclusions

A quantitative parameter, displacement change of indenter ( $\Delta h$ ) during the holding process in unloading, is proposed for in situ characterization of the formation and growth of nanoindentation-induced high-pressure phases of silicon. For the same maximum indentation load,  $\Delta h$  tends to increase with the decrease in the holding load  $\Delta P$  and increase with the increase in the loading/unloading rate if no pop-out occurs before or during the holding process.

After the pop-out event,  $\Delta h$  becomes stable. Results also indicate that the initial nucleation of high-pressure phases is pressure dependent. When pressure is released to a critical value, small volumes of Si-XII/Si-III phases seed within the Si-II phase even though the unloading rate is very fast. If a holding process is given during very fast unloading, high-pressure phases further grow, leading to occurrence of a pop-out. This study demonstrates that  $\Delta h$  may be used to predict the formation and growth of nanoindentation-induced high-pressure phases, especially the initial nucleation of high-pressure phases, and thus provide useful information for preparing Si-XII/Si-III phases through high-pressure techniques.

**Acknowledgments** H.H. is an International Research Fellow of the Japan Society for the Promotion of Science (JSPS). This study has been financially supported by Grant-in-Aid for JSPS Fellows (Grant No. 26-04048) and Grant-in-Aid for Exploratory Research (Grant No. 15K13838).

## References

1. L. Rapp, B. Haberl, C.J. Pickard, J.E. Bradby, E.G. Gamaly, J.S. Williams, A.V. Rode, *Nat. Commun.* **6**, 7555 (2015)
2. P.C. Verburg, L.A. Smillie, G.R.B.E. Romer, B. Haberl, J.E. Bradby, J.S. Williams, A.J.H. in't Veld, *Appl. Phys. A Mater. Sci. Process.* **120**(2), 683 (2015)
3. S. Zhao, E.N. Hahn, B. Kad, B.A. Remington, C.E. Wehrenberg, E.M. Bringa, M.A. Meyers, *Acta Mater.* **103**, 519 (2016)
4. D.J. Sprouster, S. Ruffell, J.E. Bradby, D.D. Stauffer, R.C. Major, O.L. Warren, J.S. Williams, *Acta Mater.* **71**, 153 (2014)
5. E. Zdanowicz, T.A. Dow, R.O. Scattergood, K. Youssef, *Precis. Eng.* **37**(4), 871 (2013)
6. S.W. Youn, C.G. Kang, *Scripta Mater.* **50**(1), 105 (2004)
7. M.I. McMahon, R.J. Nelmes, *Phys. Rev. B* **47**(13), 8337 (1993)
8. G.A. Voronin, C. Pantea, T.W. Zerda, L. Wang, Y. Zhao, *Phys. Rev. B* **68**(2), 020102 (2003)
9. J.I. Jang, M.J. Lance, S.Q. Wen, T.Y. Tsui, G.M. Pharr, *Acta Mater.* **53**(6), 1759 (2005)
10. I. Zarudi, J. Zou, L.C. Zhang, *Appl. Phys. Lett.* **82**(6), 874 (2003)
11. Z.D. Zeng, Q.S. Zeng, W.L. Mao, S.X. Qu, *J. Appl. Phys.* **115**(10), 103514 (2014)
12. V. Domnich, Y. Gogotsi, S. Dub, *Appl. Phys. Lett.* **76**(16), 2214 (2000)
13. Y.B. Gerbig, S.J. Stranick, R.F. Cook, *Phys. Rev. B* **83**(20), 205209 (2011)
14. N. Fujisawa, S. Ruffell, J.E. Bradby, J.S. Williams, B. Haberl, O.L. Warren, *J. Appl. Phys.* **105**(10), 106111 (2009)
15. Y.H. Lin, T.C. Chen, *Appl. Phys. A Mater. Sci. Process.* **92**(3), 571 (2008)
16. R.O. Piltz, J.R. Maclean, S.J. Clark, G.J. Ackland, P.D. Hatton, J. Crain, *Phys. Rev. B* **52**(6), 4072 (1995)
17. J. Crain, G.J. Ackland, J.R. Maclean, R.O. Piltz, P.D. Hatton, G.S. Pawley, *Phys. Rev. B* **50**(17), 13043 (1994)
18. I. Zarudi, L.C. Zhang, J. Zou, T. Vodenitcharova, *J. Mater. Res.* **19**(1), 332 (2004)
19. J.W. Yan, K. Syoji, T. Kuriyagawa, H. Suzuki, *J. Mater. Process. Tech.* **121**(2–3), 363 (2002)
20. B.D. Malone, J.D. Sau, M.L. Cohen, *Phys. Rev. B* **78**(16), 161202 (2008)

21. B.D. Malone, J.D. Sau, M.L. Cohen, *Phys. Rev. B* **78**(3), 035210 (2008)
22. J.M. Besson, E.H. Mokhtari, J. Gonzalez, G. Weill, *Phys. Rev. Lett.* **59**(4), 473 (1987)
23. S. Wippermann, M. Voros, D. Rocca, A. Gali, G. Zimanyi, G. Galli, *Phys. Rev. Lett.* **110**(4), 046804 (2013)
24. B. Haberl, L.B.B. Aji, J.S. Williams, J.E. Bradby, *J. Mater. Res.* **27**(24), 3066 (2012)
25. A.P. Gerk, D. Tabor, *Nature* **271**(5647), 732 (1978)
26. J.E. Bradby, J.S. Williams, J. Wong-Leung, M.V. Swain, P. Munroe, *Appl. Phys. Lett.* **77**(23), 3749 (2000)
27. V. Domnich, Y. Gogotsi, *Rev. Adv. Mater. Sci.* **3**(1), 1 (2002)
28. J.W. Yan, H. Takahashi, X.H. Gai, H. Harada, J. Tamaki, T. Kuriyagawa, *Mat. Sci. Eng. A Struct.* **423**(1–2), 19 (2006)
29. S. Ruffell, J.E. Bradby, J.S. Williams, P. Munroe, *J. Appl. Phys.* **102**(6), 063521 (2007)
30. T. Juliano, Y. Gogotsi, V. Domnich, *J. Mater. Res.* **18**(5), 1192 (2003)
31. P.S. Pizani, R.G. Jasinevicius, A.R. Zanatta, *Appl. Phys. Lett.* **89**(3), 031917 (2006)
32. R.G. Jasinevicius, J.G. Duduch, P.S. Pizani, *Semicond. Sci. Tech.* **22**(5), 561 (2007)
33. Y. Gogotsi, C. Baek, F. Kirscht, *Semicond. Sci. Tech.* **14**(11), 936 (1999)